IEEE Access
Multidisciplinary | Rapid Review | Open Access Journal

Received October 5, 2020, accepted October 27, 2020, date of publication October 30, 2020, date of current version November 13, 2020.

Digital Object Identifier 10.1109/ACCESS.2020.3034945

Pin Addressing Method Based on an SVM With a Reliability Constraint in Digital Microfluidic Biochips

JINLONG SHI, PING FU, (Member, IEEE), AND WENBIN ZHENG, (Member, IEEE)
School of Electronics and Information Engineering, Harbin Institute of Technology, Harbin 150080, China

Corresponding author: Wenbin Zheng (zhengwenbin@hit.edu.cn)

This work was supported in part by the Heilongjiang Postdoctoral Fund (Grant No. LBH-Z16081).

ABSTRACT Digital microfluidic biochips (DMFBs) are increasingly important and are used for point-of-care, drug discovery, clinical diagnosis, immunoassays, etc. Pin-constrained DMFBs are an important part of digital microfluidic biochips, and they have gained increasing attention from researchers. However, many previous works have focused on the problem of electrode addressing and aimed to minimize the number of control pins in pin-constrained DMFBs. Although the number of control pins can be effectively redistributed through broadcast addressing technology, the chip reliability will be reduced if the signals are shared arbitrarily. Arbitrary signal sharing can lead to a large number of actuations for many idle electrodes, and as a result, a trapping charge or decreasing contact angle problem could occur for some electrodes, reducing the reliability of the chip. To address this problem, the appropriate electrode matching object should be carefully selected, and the influence of these factors on chip reliability should be fully considered. For this purpose, we aimed to fully consider electrode addressing and the reliability of the chip in improving the reliability of DMFBs. This paper proposed a pin addressing method based on a support vector machine (SVM) with the reliability constraint algorithm, which can fully consider the electrode addressing method and the reliability of the chip together. The proposed method achieved an average maximum number of electrode actuations that was 53.8% and 18.2% smaller than those of the baseline algorithm and the graph-based algorithm, respectively. The simulation experiment results showed that the proposed method can efficiently solve reliability problems during the DMFB design process.

INDEX TERMS Digital microfluidic biochips, pin assignment, reliability, actuation times, SVM.

I. INTRODUCTION

Clinical diagnosis is an important link in disease diagnosis [1]. Traditional clinical disease detection usually relies on large testing equipment at a testing center, which not only takes a long time to detect diseases but also consumes a large amount of reagents and attracts great controversy due to the need to collect many biological specimens such as blood [2]. With continuing innovations in manufacturing and packaging processes, modern microelectromechanical systems (MEMSs) and microfluidic systems are being applied to combine many chemical, mechanical, or electrical devices into a single package [3]–[7]. A microfluidic chip can provide detection results in a short time by using a small number of samples, and it has a high detection sensitivity, good specificity, a simple operation process and short cycles; it has become one of the best solutions to the current problem [8]. Many traditional biological programs can be implemented efficiently in digital microfluidic systems by applying a prescheduled electrical drive sequence to control the micro-, nano- or pico-liter volume of droplets [9]. Therefore, microfluidic biochips have the ability to substitute for traditional laboratory equipment, as they integrate all the necessary functions to complete a bioassay [10], [11]. Biochips are being applied in many areas, such as point-of-care clinical diagnostics, drug discovery, protein analysis and immunoassays [12]–[15]. DMFBs use discrete droplets to perform operations such as dispensing, transport, mixing, splitting and detection. The basic droplet movement is based on the electrowetting on dielectric (EWOD) principle [16], [17]. Hence, the operations can be executed anywhere on the chip by occupying a set of electrodes in a reconfigurable way.

The associate editor coordinating the review of this manuscript and approving it for publication was Agustin Leobardo Herrera-May.

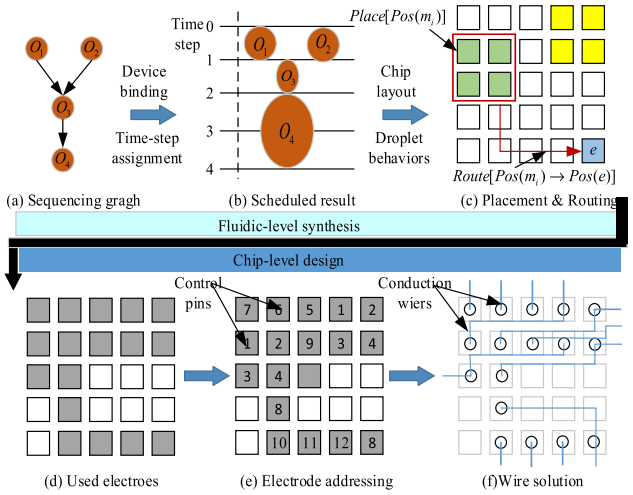

FIGURE 1. (a) The sequential graph of a bioassay. (b) The schedule result of a bioassay. (c) The placement and routing result. (d) The used electrode results. (e) The design results of electrode addressing. (f) The design results of wire routing.

The design process for DMFBs is shown in Figure 1, which consists of two main stages: fluidic-level synthesis and chip-level design. In the past decade, there have been notable advances in computer-aided design methodology for fluidic-level synthesis, including resource binding, operation scheduling, module placement, chip washing and functional droplet routing. The typical objectives are to minimize the assay execution time and the number of used cells so that the number of driving electrodes can be minimized for power and interconnection savings. The chip-level design is also of great importance, as it directly determines the fabrication cost and reliability of the DMFBs. The sequential graph of a bioassay in Figure 1(a) is synthesized onto a given sized chip and the schedule result is shown in Figure 1(b). The placement and routing results are shown in Figure 1(c). The used electrode results are shown in Figure 1(d). Figure 1(e) and 1(f) show the design results of electrode addressing and of wire routing, respectively.

At present, digital microfluidic biochips have attracted increasing attention and have been applied in many areas. In the process of chip design, all electrodes should be connected to their corresponding control pins; this process is called electrode addressing or pin assignment [18]. The purpose of pin addressing is to receive control signals from external controllers for the correct drive electrode. In the conventional pin allocation scheme for a chip, each electrode is controlled with an independent control pin; this is called direct addressing [19]. In the direct addressing scheme, each electrode can be controlled independently. As the complexity of the biological and chemical analysis implemented on the chip and the chip size increase, the scale of the chip also increases [20]. However, the numbers of external controller pins and signal ports are limited; hence, it is necessary to limit the number of control pins [21]. The broadcast addressing method, which is widely used for pin allocation, was proposed to address this problem [22]. Broadcast addressing utilizes the concept of pin sharing to assign an individual control pin to multiple electrodes without affecting the execution and analysis of the biochemical experimental processes. Therefore, broadcast addressing can effectively reduce the number of control pins during the DMFB design process.

In the literature, there are many previous works focusing on the design of pin-constrained DMFBs. Many previous works focus only on the problem of electrode addressing and aim to minimize the number of control pins [23]–[28]. Reference [27] focuses on pin count minimization for general-purpose DMFBs and presents a pin count minimization algorithm based on sophisticated electrode chaining for regular and irregular electrode arrays. The key idea of the proposed method is that actuation information can be transmitted from previous neighborhood electrodes to later ones in a chain. Some essential sufficient pin assignment architecture for pin-constrained DMFBs and a pin assignment technique for multifunctional biochips are presented in [28] to solve the pin reduction problem.

Although the number of control pins can be effectively redistributed through broadcast addressing technology, the chip reliability will be reduced if the signals are shared arbitrarily [29]. In the design process for a broadcast addressing chip, arbitrary signal sharing can lead to a large amount of switching for many idle electrodes; as a result, the trapping charge or decreasing contact angle problem could occur for some electrodes [30], [31]. Thus, in order to deal with the reliability problem, when electrodes are assigned to the same control pin, the appropriate electrode matching object should be carefully selected, and the influence of these factors on chip reliability should be fully considered.

Many works consider both electrode addressing and the reliability problem. Reference [32] presented the first matching-based reliability-oriented broadcast addressing algorithm for DMFBs. This algorithm identifies the factors that affect reliability and incorporates them into the design technique attributes that enhance reliability and make the DMFBs more feasible in practical applications. Reference [33] presents a network-flow-based algorithm for reliability-driven pin-constrained DMFBs. The proposed algorithm not only minimizes the reliability problem induced by signal merging but also prevents operational failures caused by inappropriate addressing results. A comprehensive routing solution is also proposed for chip-level DMFB designs in reference [33]. References [34], [35] present a graph-based chip-level design algorithm. By setting the switching-time constraint, the switching times can be limited to minimize the impact of the contact angle change reduction problem. The reliability and electrode addressing problems are considered in the chip-level design of DMFBs, and a progressive addressing and routing approach are proposed to overcome the complex wire-routing problem. However, the reliability of the chip is not fully considered in the design of the chip. Prior works consider only the effect on reliability of the trapping charge or the contact angle change reduction, but not the effect of both of them together. Furthermore,

in this paper, we aim to fully consider the electrode addressing and the reliability of the chip for improving the reliability of DMFBs during the design process.

Prior work on the pin addressing problem has typically modeled it as clique partitioning problem on a compatibility graph [36]. Each clique of electrodes in the graph represents a potential pin group, that is, a group of electrodes that can share the same control pin and all of whose electrode actuation sequences are mutually compatible. The general clique partitioning problem is an NP-hard problem [37], [38] and has been a popular research topic in many areas. Tomita proved that the time complexity of enumerating maximal cliques is $O(3^{n/3})$ in the worst case in any graph with n nodes and m edges because in a graph of n vertices, there are at most $3^{n/3}$ maximal cliques [39].

With the great success of machine learning methods in computer vision [40], natural language processing [41], biometric identification [42], medical diagnosis [43], DNA sequencing [44] and other fields, researchers have tried to use machine learning methods to solve problems in the design process of digital microfluidic chips [45]. The goal of machine learning is to learn a function that is well adapted to "new samples" and "new environments" [46]. Therefore, compared with traditional methods, the machine learning-based digital microfluidic chip design method can better adapt to dynamic changes in the design environment (such as changes in the chip size, electrode occupation and application environment) and various performance index optimization requirements during the chip design process. Therefore, the design method of digital microfluidic chips based on machine learning shows great potential in the chip design process. Arbitrary signal sharing can lead to a large number of actuations for many idle electrodes; the appropriate electrode matching object should therefore be selected carefully, and the influence of these factors on chip reliability should be fully considered. For this purpose, we aim to fully consider the electrode addressing process and the reliability of the chip for improving the reliability of DMFBs. This paper proposes a pin addressing method based on an SVM with a reliability constraint, which can fully consider electrode addressing and the reliability of the chip together during the DMFB design process.

The rest of this paper is organized as follows: Section II presents electrode addressing in pin-constrained DMFB designs and formulates the pin addressing problem. Section III presents an overview of the proposed SVM algorithm, and Section IV describes the proposed SVM algorithm in detail to solve the practical pin addressing problem. Sections V and VI describe the experimental results and conclude the paper, respectively.

II. SYSTEM MODEL

A. PROBLEM FORMULATION

Broadcast addressing utilizes the concept of pin sharing to assign an individual control pin to multiple electrodes without affecting the execution or analysis of biochemical experimental processes. Figure 2(a) and (b) show an electrode set and the corresponding actuation sequences. Two electrode actuation sequences are compatible if either the values of the two bits are the same at every time step or the value of one bit is "X". Specifically, we can replace the status "X" with "1" or "0", and therefore, different actuation sequences become identical sequences. For example, let the actuation sequences of electrodes e_6 and e_8 be $X00001$ and $10000X$, respectively. We can obtain the same result of 100001 by replacing each "X" in the actuation sequences of e_6 and e_8 with one. Therefore, because the actuation sequences of e_6 and e_8 are compatible, the same control pins can be processed for both. Broadcast addressing aims to find electrode groups with compatible actuation sequences and assign a dedicated control pin to each group; that is, one control pin can control multiple electrodes, thereby reducing the total pin count required for pin assignment without affecting the bioassay operation. During pin assignment, broadcast addressing is usually modeled as a compatibility graph in which a vertex represents an electrode and an edge between two electrodes indicates that they are compatible with each other. Therefore, the derivation of a broadcast addressing result can be mapped to a graph problem of clique partitioning. The equivalent graph is split into five parts, as shown in Figure 2(d), and the broadcast addressing results are as shown in Figure 2(c). With broadcast addressing, the pin count needed to control a bioassay can be dramatically reduced.

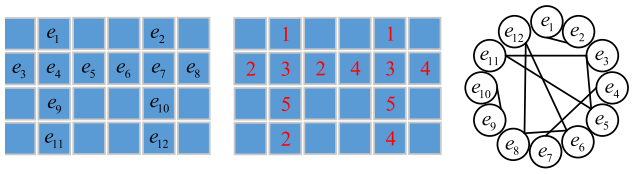

Electrode	e_1	e_2	e_3	e_4	e_5	e_6	e_7	e_8	e_9	e_{10}	e_{11}	e_{12}
Actuation Sequence	0	0	1	0	X	X	0	1	0	0	X	X
	0	0	1	1	1	0	1	0	0	0	1	X
	1	1	0	1	0	0	1	0	1	1	0	0
	1	1	1	0	1	0	0	0	0	0	1	0
	0	0	0	1	0	0	1	0	0	0	X	X
	0	0	X	0	1	1	0	X	0	0	X	X

(b)

FIGURE 2. (a) Electrodes used for biochemical experimental processes. (b) Actuation sequences of biochemical experimental processes. (c), (d) Broadcast addressing result and corresponding clique-partition result in a compatibility graph.

Although the number of control pins can be effectively redistributed through broadcast addressing technology, the chip reliability will be reduced if the signals are shared arbitrarily. In the design of a broadcast addressing chip, arbitrary signal sharing can lead to a large amount of switching for many idle electrodes, and as a result, the trapping charge or decreasing contact angle problem could occur for some electrodes, thus reducing the reliability of the chip. For example, in Figure 3, there are three electrodes, e_1, e_2 and e_3, and their corresponding actuation sequences are $s_1 = 10 \times 0 \times 0$,

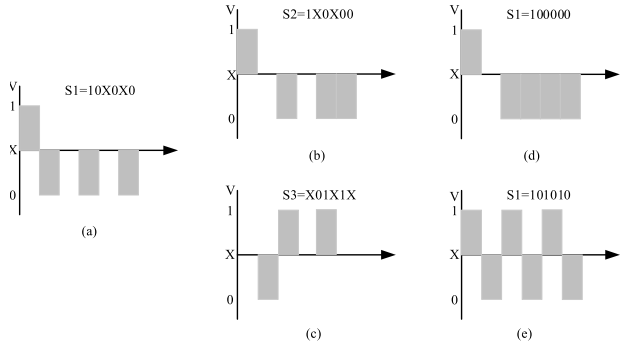

FIGURE 3. s_1, s_2 and s_3 are the actuation sequences of electrodes e_1, e_2 and e_3, as shown in (a), (b) and (c), respectively. The number of actuations of electrode e_1 is one in the first case, as shown in (d). The number of actuations of electrode e_1 is three in the second case, as shown in (e).

$s_2 = 1\times0\times00$ and $s_3 = X01\times1X$, respectively. According to these actuation sequences, electrode e_1 can share a control pin with e_2, or e_1 can share a control pin with e_3. Although both broadcast addressing results are same in terms of the number of control pins reduced, the number of actuations varies greatly for electrode e_1. In the first case, if electrode e_1 shares a control pin with e_2, the actuation sequence of electrode e_1 becomes $s_1 = 100000$, and the number of actuations of e_1 is one. However, in the second case, if electrode e_1 shares a control pin with e_3, the actuation sequence of electrode e_1 becomes $s_1 = 101010$, and the number of actuations of e_1 is three. The number of actuations in the second case is greater than that in the first case, and the maximum number of actuations must be taken into consideration when performing broadcast addressing. Thus, our optimization objective is to minimize the maximum number of actuations of all electrodes in performing broadcast addressing.

B. APPLICATION MODEL

The problem of electrode addressing and the reliability of the DMFBs during the design process can be formulated as follows: The set of electrodes used for biochemical experimental processes is modeled as $E = \{e_1, e_2, \cdots, e_n\}$, where e_i represents the ith electrode and n represents the number of electrodes. The corresponding actuation sequences of E are represented by $S = \{s_1, s_2, \cdots s_n\}$. The constraint on the number of pins is defined as $P_{\max}$. The set of pins used for the biochemical experimental processes is defined as $P = \{p_1, p_2, \cdots p_m\}$, where m represents the number of pins, so the constraint on the number of pins can be represented by equation (1).

$$m \le P_{\max} \tag{1}$$

To ensure that the pin assignment is determined correctly, each electrode $e_i \in E$, $1 \le i \le n$, must be assigned to exactly one pin $p_j \in P$, $1 \le j \le m$. The set of electrodes controlled by pin p_j is defined as Ep_j, where electrodes e_k and e_l belong to Ep_j. That is, $\forall e_k \in Ep_j$ and $\forall e_l \in Ep_j$, $1 \le k \le n$, $1 \le l \le n$. To determine the compatibility of an electrode sequence, we define rules such as $1 \,\&\, X = 1$, $X \,\&\, X = 1$ and $0 \,\&\, X = 1$, and the broadcast addressing constraints are represented by equation (2).

$$s_k \,\&\, s_l = 1 \tag{2}$$

As mentioned above, the electrode addressing and reliability problems can be solved by reducing the number of electrode drives during the DMFB design process. Therefore, the global effect of reliability can be reduced by minimizing the maximum number of actuations of e_i. We define the value "1" in the electrode actuation sequence to represent that the electrode is actuated; then, the number of activations of electrode $e_i \in E$ can be expressed as equation (3).

$$St_i = \sum_{t=1}^{step} S_i(t), \quad \forall e_i \in E, \tag{3}$$

where St_i represents the number of activations of electrode e_i and step represents the number of time steps in a sequence. In this paper, we aim to fully consider electrode addressing and the reliability of the chip for improving the reliability of DMFBs during the design process. Consequently, this paper can average the number of actuations of electrodes to achieve good chip reliability. The objective formula used in this research can be defined as equation (4).

$$D = \min(\sum_{i=1}^{n} (St_i - \frac{\sum_{i=1}^{n} St_i}{n})^2 \tag{4}$$

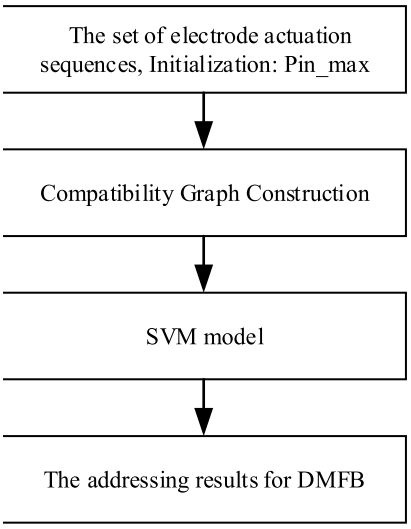

FIGURE 4. Overview of the pin addressing method based on an SVM with a reliability constraint.

III. OVERVIEW

We propose a pin addressing method based on an SVM with a reliability constraint in this study. This section provides a detailed description of the algorithm. First, we briefly introduce the whole procedure, as shown in Figure 4. The components and functions of the proposed algorithm are introduced

in three subsections, including (1) the initialization of the algorithm, (2) the constrained compatibility graph construction, and (3) the pin addressing method based on the SVM. Figure 4 shows an overview of our pin addressing method based on an SVM with a reliability constraint. First, the set of electrode actuation sequences is taken as input, and the constraint on the maximum number of pins is set as $P_{\max}$. Then, the compatibility graph of all electrodes is constructed, and the reliability constraint is fully considered. Finally, the addressing results for the DMFB are obtained by the pin allocation method based on the SVM.

A. COMPATIBILITY GRAPH CONSTRUCTION

When applying broadcast addressing, an essential task is grouping the set of electrodes such that all electrodes in the same group are mutually compatible. Then, a compatibility graph $G(V, O)$ is constructed, where the vertex set V represents the electrode set and the edge set O between two electrodes indicates that their corresponding actuation sequences are compatible. Note that compatibility is examined for both identical and complementary signals.

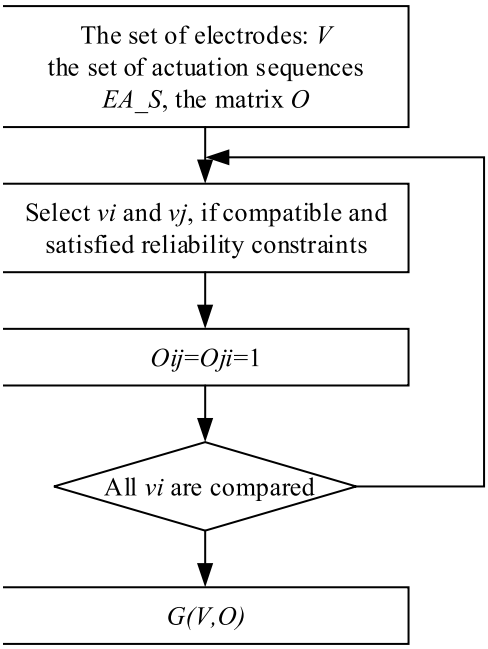

FIGURE 5. The process of compatibility graph construction.

According to the set of actuation sequences EA_S, a compatibility graph is constructed as shown in Figure 5. First, a compatibility graph node is constructed, which represents the current selected electrode v_i. Then, the actuation sequence of the selected electrode is compared with the actuation sequence of another electrode v_j in the set of actuation sequences; if the electrodes can be actuated using the same actuation sequence, the new electrode is added to the compatibility graph and a side line is added between the electrodes to form the adjacency matrix $O_{ij} = O_{ji} = 1$. The side line between the electrodes represents that the actuation sequences between the electrodes are compatible. The compatibility diagram can be constructed by comparing the actuation sequences of each electrode with those of other electrodes in the set of electrodes and drawing the lines one by one.

B. THE PRINCIPLE OF THE SVM

In this paper, a pin addressing method is proposed, and the core idea of our prediction model is based on an SVM. The fundamental principle of the SVM is shown in Figure 6.

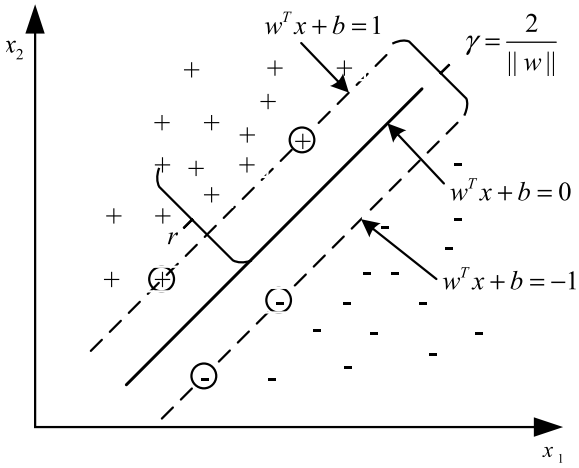

FIGURE 6. The fundamental principle of the support vector machine.

Given a training set $D = \{(x_1, y_1), (x_2, y_2), \cdots, (x_m, y_m)\}$, classification learning aims to find a partition hyperplane in the sample space and then separate the samples into different categories. In the sample space, the partition hyperplane can be described by the following equation:

$$w^T x + b = 0, \tag{5}$$

where $w = (w_1; w_2; \cdots; w_d)$ is the normal vector and determines the direction of the hyperplane; b is the displacement, which determines the distance between the hyperplane and the origin. Clearly, the partition hyperplane can be determined by the normal vector W and the displacement B, and it is denoted as (w, b). The distance from any point x in the sample space to the hyperplane can be expressed as

$$r = \frac{|w^T x + b|}{||w||}. \tag{6}$$

If the hyperplane (w, b) can correctly classify the training samples—that is, for $(x_i, y_i) \in D$, if the equation $y_i = +1$ holds—then $w^T x + b > 0$. If $y_i = -1$, then the equation $w^T x + b < 0$ holds. This establishes equation (7).

$$\begin{cases} w^T x_i + b \geq +1, & y_i = +1 \\ w^T x_i + b \leq -1, & y_i = -1 \end{cases} \tag{7}$$

As shown in Figure 7, the equals sign of equation (7) is established by the training sample points closest to the hyperplane, which are called the "support vectors". The sum

of the distances between two heterogeneous support vectors and the hyperplane can be expressed as:

$$\gamma = \frac{2}{||w||} \tag{8}$$

where γ is called the margin.

To find the partition hyperplane with the "maximum margin", the parameters W and B that satisfy the constraints in equation (7) should be found that make γ maximal, namely:

$$\begin{cases} \max\limits_{w,b} \dfrac{2}{||w||} \\ s.t.\ y_i(w^T x_i + b) \geq 1, \quad i = 1, 2, \ldots, m. \end{cases} \tag{9}$$

Clearly, in order to maximize the margin, we only need to maximize $||w||^{-1}$, which is equivalent to minimizing $||w||^2$, so equation (9) can be rewritten as:

$$\begin{cases} \min\limits_{w,b} \dfrac{1}{2}||w||^2 \\ s.t.\ y_i(w^T x_i + b) \geq 1, \quad i = 1, 2, \ldots, m. \end{cases} \tag{10}$$

Equation (9) is the basic model of an SVM.

IV. ALGORITHM IMPLEMENTATION

In the overall flow of the pin addressing method based on an SVM with the reliability constraint method, an important step is the generation of SVM-based models.

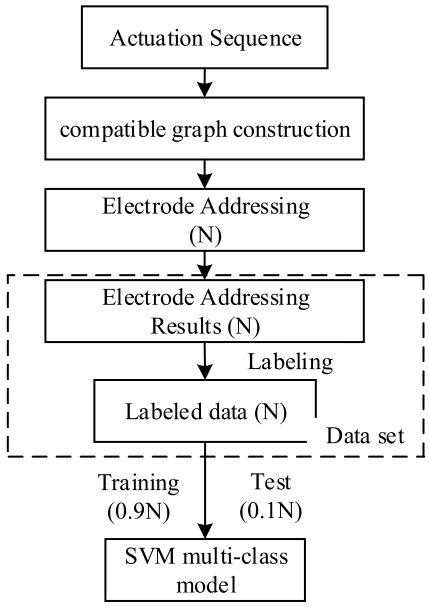

FIGURE 7. The flow of the training step in the SVM-based electrode addressing method.

A. SVM-BASED MODELS

Figure 7 presents the flow of the training step in the SVM-based electrode addressing method. In this flow, first, a compatibility graph is generated according to the electrode drive sequence, and a set of pin addressing solutions is randomly generated according to the compatibility graph. Then, the SVM features for each pin addressing solution are extracted as a part of the training set. When the SVM features for each pin addressing solution are extracted, the pin addressing solutions are labeled according to equation (11). We use equation (11) to evaluate the quality of each pin addressing solution. In addition, we classify the quality of the electrode pin addressing solutions into several levels. The training set is thereby obtained for the SVM classifier. Finally, we learn an SVM multiclass classifier based on the training set using the SVM kernel in [38].

B. FEATURE EXTRACTION

Feature extraction is one of the most important steps in an approach based on machine learning. In this study, we use two pin assignment attributes as the feature vectors, the number of pins CP, and the variance of the number of electrode actuations D to obtain a pin addressing solution.

C. EVALUATION SCORE

To deal with the pin-constraint problem of DMFBs, we use a feature CP. The feature CP represents the number of control pins in a pin addressing solution. The smaller the value of CP is, the higher the quality of the pin addressing solution of the chip. To deal with the reliability problem of DMFBs, we use a feature D. The feature D presents the variance of the number of actuations of all the electrodes in a pin addressing solution. The smaller the value of variance D is, the higher the reliability of the chip. The feature D appears in the definition of a reliability problem, which is computed by equation (4).

After the pin addressing stage, we define a function $Score$ to evaluate the quality of a pin addressing solution as follows:

$$Score = \frac{R}{CP + D} \cdot TE \cdot TC \tag{11}$$

where R is a user-defined parameter, which is acquired through experiment and experience; the parameters TE and TC are used for normalization, the parameter TE is the total number of electrodes for the benchmark, and the parameter TC is the total area of a chip.

V. SIMULATION AND RESULTS

The SVM algorithm was applied to the pin-constrained design of biochips as a protein assay representative, a multiplexed immunoassay, and the polymerase chain reaction (PCR) procedure in this paper. First, all of the experiments were mapped to a chip with 15×15 and 13×21 electrode arrays by direct addressing for pin assignment, then the driver sequences of all electrodes were obtained. Then, according to the driving sequence of each electrode, the proposed SVM method was used to reduce the number

of control pins and assess the reliability of the chip. Finally, we evaluated the proposed method for pin-constrained design by simulation for these bioassays.

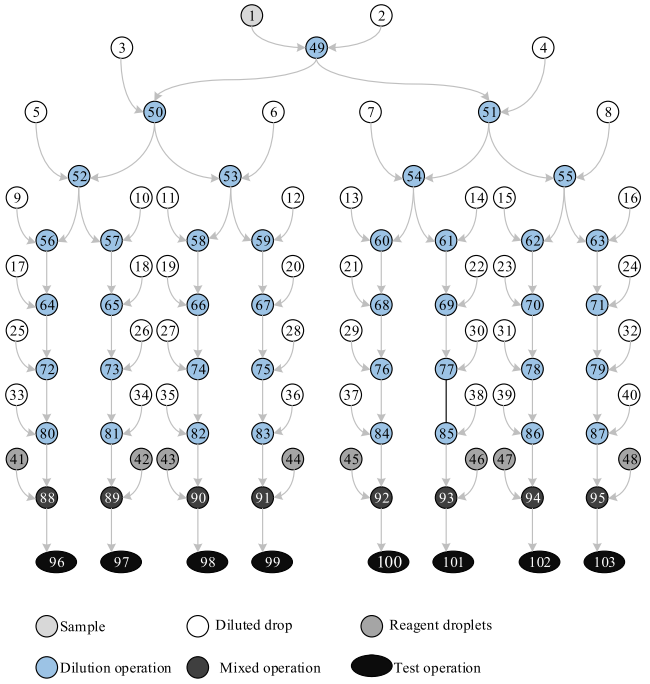

FIGURE 8. Sequence diagram of the protein analysis experiment.

A. EXPERIMENTS

1) PROTEIN ANALYSIS EXPERIMENT

We mapped the protein assay to the 13 × 21 array. Figure 8 shows the operational sequence diagram of the protein analysis experiment. There were 103 operating nodes in total; the first node represented the sample droplet, operations 2 to 40 represented the buffer droplets, operations 41 to 48 represented the reagent droplets, operations 49 to 87 represented the dilution operation, operations 88 to 95 represented mixed operations, and operations 96 to 103 represented the optical detection operation.

2) MULTIPLEXED EXPERIMENT

We mapped the multiplexed experiment to the 15 × 15 array. The multiplexed experiment was composed of a glucose assay and a lactate assay based on colorimetric enzymatic reactions. The sequencing graph of the multiplexed experiment is shown in Figure 9. Two sample droplets and two reagent droplets are dispensed into the chip. They consisted of four pairs of droplets to be mixed, $\{S_1, R_1\}$, $\{S_1, R_2\}$, $\{S_2, R_1\}$, and $\{S_2, R_2\}$. Finally, the analysis was completed by sequencing at the detection site.

3) POLYMERASE CHAIN REACTION

A PCR is a molecular biology technique used to amplify specific DNA fragments, which can be regarded as specific

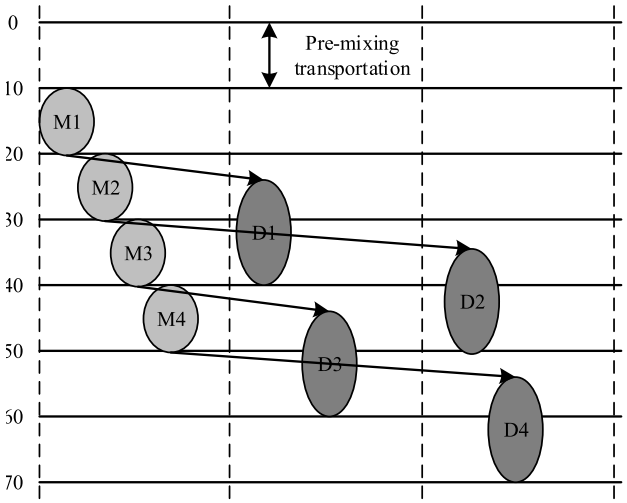

FIGURE 9. Schedule result for the multiplexed bioassay.

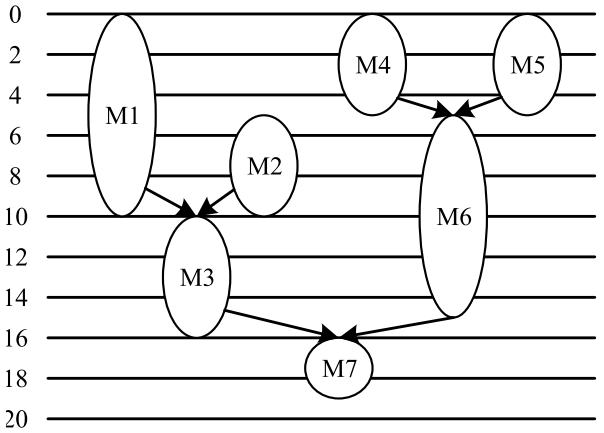

FIGURE 10. The schedule for the PCR assay.

DNA replication in vitro. We also mapped the PCR to the 15 × 15 array; the sequencing graph of the PCR is shown in Figure 10. These stages are used for rapid enzymatic amplification of specific DNA strands, and this process consists of seven mixed operations. The feasibility of performing droplet-based PCR on digital microfluidics-based biochips has been demonstrated.

B. THE SIMULATION RESULTS

To evaluate the performance of our methods, the simulation was implemented on MATLAB R2015a. Table 1 lists the experiment specifications, including the size of the chip, the number of electrodes, the time steps of the assay and the number of pin constraints.

To verify the effectiveness of the proposed algorithm in reducing the numbers of pins and electrode actuations, this paper compares our experimental results with the baseline algorithm and the graph-based algorithm [27] in Table 2. For the above three bioassays, we compare the electrode

TABLE 1. The statistics of all experiments.

Benchmark	Size	Electrodes	Time step	P_{max}
Protein analysis	13*21	77	106	32
Multiplexed	15*15	59	70	32
PCR	15*15	62	20	32

TABLE 2. The simulation results of different size of DMFBs.

Bench mark	Baseline[34]			graph-based[34]			SVM		
	Np	ACT-max	CPU (s)	Np	ACT-max	CPU (s)	Np	ACT-max	CPU (s)
Multip	22	9	26.3	24	4	29.23	28	3	35.4
PCR	28	8	23	30	6	92.55	32	5	106.8
Protein	27	22	30.13	32	12	98.85	32	10	138.6
average	25.6	13	26.5	28.7	7.33	73.5	30.67	6	93.6

addressing results with the number of control pins (Np), the maximum number of electrode actuations (ACTm), and the CPU running time (CPU) for the three-pin addressing method. Table 2 shows the experimental results obtained from our proposed algorithm. Column 1 lists the three kinds of experiment: protein, multiplexed, and PCR. Columns 2, 3 and 4 show the experimental results obtained by the baseline algorithm. Columns 5, 6 and 7 show the experimental results obtained by graph-based algorithm. Columns 8, 9 and 10 show the experimental results of our study.

The experimental results are shown in Table 2. The improvements in reducing the number of pins, the maximum number of electrode actuations and the CPU time are shown in the average rows. Although the CPU running time of the proposed algorithm is longer and the average number of control pins (Np) is greater than those of the baseline algorithm and the graph-based algorithm, the performance in terms of the maximum number of electrode actuations of the proposed algorithm is much better than those of the baseline algorithm and the graph-based algorithm. As shown in Columns 2-4, although the results of the baseline algorithm satisfy the design specifications, the experimental results of our proposed algorithm, shown in Columns 8-10, are much better than those of the baseline algorithm. The proposed algorithm can achieve an average maximum number of electrode actuations (ACTmax) that is 53.8% and 18.2% less than those of the baseline algorithm and the graph-based algorithm. The experimental results provide powerful evidence for the practicability of the SVM algorithm that was proposed in this paper.

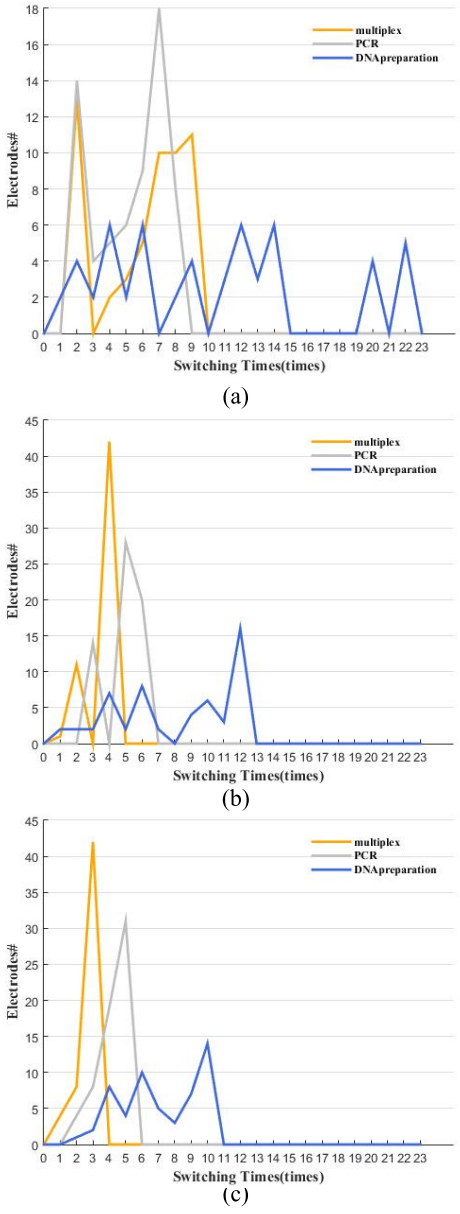

FIGURE 11. Distribution of the numbers of electrodes and electrode activations. (a) The baseline method; (b) the graph-based method; (c) ours.

To further evaluate the reliability, the distribution of the electrode actuations in the three verification tests is shown in Figure 11.

The distributions of the number of electrodes and electrode actuations of the baseline algorithm are shown in Figure 11(a). For the baseline algorithm, a large number of electrodes are actuated many times; the maximum number of electrode actuations in the multiplex test, PCR, and DNA preparation are nine, eight, and twenty-two, respectively, indicating that many electrodes suffer from a reliability problem. In addition, the distributions of the number of electrodes and electrode actuations for the graph-based algorithm are shown in Figure 11(b). The maximum number

of electrode actuations for the multiplex test, PCR, and DNA preparation are four, six, and twelve, respectively. This is an improvement over the baseline algorithm, but the maximum number of electrode actuations in the tests is still high, indicating that many electrodes may still suffer from the reliability problem. On the other hand, the distribution of electrode actuations for the proposed algorithm is shown in Figure 11(c). The maximum number of electrode actuations in the multiplex test, PCR, and DNA preparation are three, five, and ten, respectively. Most electrodes are actuated a small number of times, indicating that the impact of the reliability problem can be controlled well by the proposed algorithm.

The reliability of the chip is an important parameter for a biochip. Thus, the number of electrode actuations needs to be considered carefully in an efficient DMFB design process. To decrease the probability of electrode breakdown, we have to reduce the number of electrode actuations. Therefore, the main objective is the minimization of the number of actuations of all electrodes during the pin addressing process. Table 2 indicates that the proposed algorithm can minimize the number of activations of all electrodes during the pin addressing process and achieve an average distribution of activations for all electrodes. Figure 12 shows the addressing and wire routing result for the 15 × 15 array of the PCR chip with 62 electrodes.

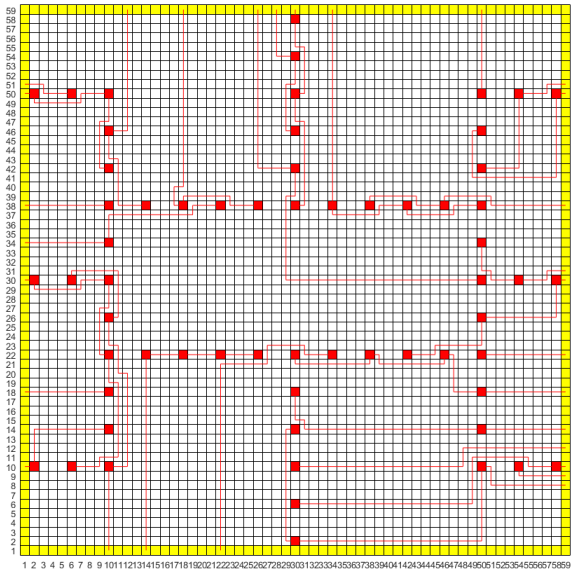

FIGURE 12. The addressing and wire routing result for the 15 × 15 array of the PCR chip with 62 electrodes.

The yellow grids around the chip represent control pins that can be wired, the red grid represents the electrodes used in the PCR experiment, and the red lines indicate wires between electrodes or between the electrodes and the external control pins. As shown in Figure 12, electrodes sharing a single control pin are successfully connected together and connected to the boundary control pins.

VI. CONCLUSION

This paper presented a novel pin addressing method based on an SVM with a reliability constraint method, which can fully consider electrode addressing and the reliability of the chip together. This study investigated the design parameters, such as the number of control pins, the maximum number of electrode actuations and the CPU running time, during the DMFB design process. Three experiments were used to evaluate the efficacy of the proposed method. The SVM algorithm was applied to the pin-constrained design of biochips for a protein assay representative, a multiplexed immunoassay, and the PCR procedure. The CPU running time of the proposed algorithm was longer and the average number of control pins was greater than those of the baseline algorithm and the graph-based algorithm. However, the performance in terms of the maximum number of electrode activations of the proposed algorithm is much better than that of the baseline algorithm and the graph-based algorithm. The proposed algorithm can achieve an average maximum number of electrode activations that is 53.8% and 18.2% less than those of the baseline algorithm and the graph-based algorithm, respectively, and the primary objective of DMFB design in this paper is achieved. The experimental results show that the proposed algorithm is much better than the baseline algorithm and graph-based algorithm and that the SVM algorithm can increase the reliability of chips. Most electrodes are actuated a small number of times, indicating that the impact of the reliability problem can be controlled well by the proposed algorithm. The good performance in terms of the simulation results provides powerful evidence for the practicability of the SVM algorithm proposed in this paper, and the simulation results are useful for the practical application of the algorithm in the future. Additionally, a real chip design method based on the SVM algorithm will be implemented on an actual microfluidic chip platform in the future. There are several important indicators that largely determine the performance of DMFBs, such as the overall chip cost, wire routing and routability. These objectives should also be optimized during the chip design process, which will be the main focus of future research.

REFERENCES

[1] P. Wang and L. J. Kricka, "Current and emerging trends in point-of-care technology and strategies for clinical validation and implementation," *Clin. Chem.*, vol. 64, no. 10, pp. 1439–1452, Oct. 2018.
[2] H.-H. Shen, S.-K. Fan, C.-J. Kim, and D.-J. Yao, "EWOD microfluidic systems for biomedical applications," *Microfluidics Nanofluidics*, vol. 16, no. 5, pp. 965–987, May 2014.
[3] S. Windh, C. Phung, D. T. Grissom, P. Pop, and P. Brisk, "Performance improvements and congestion reduction for routing-based synthesis for digital microfluidic biochips," *IEEE Trans. Comput.-Aided Design Integr. Circuits Syst.*, vol. 36, no. 1, pp. 41–54, Jan. 2017.
[4] V. Shukla, F. A. Hussin, N. H. Hamid, and N. B. Z. Ali, "Advances in testing techniques for digital microfluidic biochips," *Sensors*, vol. 17, no. 8, pp. 1719–1741, 2017.

[5] O. Ulkir, "Design and fabrication of an electrothermal MEMS microactuator with 3D printing technology," *Mater. Res. Express*, vol. 7, no. 7, 2020, Art. no. 075015.

[6] I. Ertugrul, "The fabrication of micro beam from photopolymer by digital light processing 3D printing technology," *Micromachines*, vol. 11, no. 5, p. 518, 2020.

[7] M. D. Rosso, C. H. Brodie, S. Ramalingam, D. M. Cabral, E. Pensini, A. Singh, and C. M. Collier, "Characterisation of graphene electrodes for microsystems and microfluidic devices," *Sci. Rep.*, vol. 9, no. 1, pp. 1–8, 2019.

[8] M. Abdelgawad, "Digital microfluidics: Automating microscale liquid handling," *IEEE Nanotechnol. Mag.*, vol. 14, no. 3, pp. 6–23, Jun. 2020.

[9] S. Chakraborty and S. Chakraborty, "A novel approach towards biochemical synthesis on cyberphysical digital microfluidic biochip," in *Proc. 30th Int. Conf. VLSI Design 16th Int. Conf. Embedded Syst. (VLSID)*, Jan. 2017, pp. 355–360.

[10] G.-R. Lu, C.-H. Kuo, and K.-C. Chiang, "Flexible droplet routing in active matrix-based digital microfluidic biochips," *ACM Trans. Des. Automat. Electron. Syst.* , vol. 23, no. 3, p. 37, 2018.

[11] G.-R. Lu, B. B. Bhattacharya, T.-Y. Ho, and H.-M. Chen, "Multi-level droplet routing in active-matrix based digital-microfluidic biochips," in *Proc. 23rd Asia South Pacific Design Autom. Conf. (ASP-DAC)*, Jan. 2018, pp. 46–51.

[12] T. Y. Ho, "Design automation for digital microfluidic biochips," *IPSJ Trans. Syst. LSI Des. Methodol.*, vol. 7, pp. 16–26, Feb. 2014.

[13] K. Chakrabarty, "Design automation and test solutions for digital microfluidic biochips," *IEEE Trans. Circuits Syst. I, Reg. Papers*, vol. 57, no. 1, pp. 4–17, Jan. 2010.

[14] A. Chakraborty, P. Datta, and R. K. Pal, "Design optimization at the fluid-level synthesis for safe and low-cost droplet-based microfluidic biochips," in *Proc. 31st Int. Conf. VLSI Design 17th Int. Conf. Embedded Syst. (VLSID)*. Washington, DC, USA: IEEE Computer Society, Jan. 2018, pp. 127–132.

[15] Z. Li, T.-Y. Ho, and K. Chakrabarty, "Optimization of 3D digital microfluidic biochips for the multiplexed polymerase chain reaction," *ACM Trans. Des. Autom. Electron. Syst.*, vol. 21, no. 2, pp. 1–27, Jan. 2016.

[16] C.-H. Kuo, G.-R. Lu, T.-Y. Ho, H.-M. Chen, and S. Hu, "Placement optimization of cyber-physical digital microfluidic biochips," in *Proc. IEEE Biomed. Circuits Syst. Conf. (BioCAS)*, Oct. 2016, pp. 448–451.

[17] Y.-H. Chen, C.-L. Hsu, L.-C. Tsai, T.-W. Huang, and T.-Y. Ho, "A reliability-oriented placement algorithm for reconfigurable digital microfluidic biochips using 3-D deferred decision making technique," *IEEE Trans. Comput.-Aided Design Integr. Circuits Syst.*, vol. 32, no. 8, pp. 1151–1162, Aug. 2013.

[18] J. McDaniel, Z. Zimmerman, D. Grissom, and P. Brisk, "PCB escape routing and layer minimization for digital microfluidic biochips," *IEEE Trans. Comput.-Aided Design Integr. Circuits Syst.*, vol. 36, no. 1, pp. 69–82, Jan. 2017.

[19] A. Abdoli and P. Brisk, "Stationary-mixing field-programmable pin-constrained digital microfluidic biochip," *Microelectron. J.*, vol. 77, pp. 34–48, Jul. 2018.

[20] Z. Li, K. Y.-T. Lai, P.-H. Yu, K. Chakrabarty, T.-Y. Ho, and C.-Y. Lee, "Structural and functional test methods for micro-electrode-dot-array digital microfluidic biochips," *IEEE Trans. Comput.-Aided Design Integr. Circuits Syst.*, vol. 37, no. 5, pp. 968–981, May 2018.

[21] K. Hu, T. A. Dinh, T.-Y. Ho, and K. Chakrabarty, "Control-layer routing and control-pin minimization for flow-based microfluidic biochips," *IEEE Trans. Comput.-Aided Design Integr. Circuits Syst.*, vol. 36, no. 1, pp. 55–68, Jan. 2017.

[22] P. Roy, S. Saha, H. Rahaman, and P. Dasgupta, "Novel wire planning schemes for pin minimization in digital microfluidic biochips," *IEEE Trans. Very Large Scale Integr. (VLSI) Syst.*, vol. 24, no. 11, pp. 3345–3358, Nov. 2016.

[23] T.-W. Huang and T.-Y. Ho, "A two-stage ILP-based droplet routing algorithm for pin-constrained digital microfluidic biochips," in *Proc. 19th Int. Symp. Phys. Design (ISPD)*, 2010, pp. 201–208.

[24] C. C.-Y. Lin and Y.-W. Chang, "ILP-based pin-count aware design methodology for microfluidic biochips," in *Proc. 46th Annu. Design Autom. Conf. (DAC)*, 2009, pp. 258–263.

[25] T. Xu and K. Chakrabarty, "Broadcast electrode-addressing for pin-constrained multi-functional digital microfluidic biochips," in *Proc. ACM/IEEE DAC*, Jun. 2008, pp. 173–178.

[26] Y. Zhao and K. Chakrabarty, "Co-optimization of droplet routing and pin assignment in disposable digital microfluidic biochips," in *Proc. Int. Symp. Phys. Design (ISPD)*, Santa Barbara, CA, USA, 2011, pp. 69–76.

[27] P. Howladar, P. Roy, and H. Rahaman, "An automated design of pin-constrained digital microfluidic biochip on MEDA architecture," in *Proc. Int. Conf. Adv. Comput., Commun. Informat. (ICACCI)*, Sep. 2016, pp. 1565–1570.

[28] Y.-C. Lei, C.-S. Hsu, J.-D. Huang, and J.-Y. Jou, "Chain-based pin count minimization for general-purpose digital microfluidic biochips," in *Proc. 21st Asia South Pacific Design Autom. Conf. (ASP-DAC)*, Jan. 2016, pp. 599–604.

[29] S. S.-Y. Liu, C.-H. Chang, H.-M. Chen, and T.-Y. Ho, "ACER: An agglomerative clustering based electrode addressing and routing algorithm for pin-constrained EWOD chips," *IEEE Trans. Comput.-Aided Design Integr. Circuits Syst.*, vol. 33, no. 9, pp. 1316–1327, Sep. 2014.

[30] T.-W. Huang, H.-Y. Su, and T.-Y. Ho, "Progressive network-flow based power-aware broadcast addressing for pin-constrained digital microfluidic biochips," in *Proc. 48th Design Autom. Conf.*, 2011, pp. 741–746.

[31] J. Tang, M. Ibrahim, K. Chakrabarty, and R. Karri, "Secure randomized checkpointing for digital microfluidic biochips," *IEEE Trans. Comput.-Aided Design Integr. Circuits Syst.*, vol. 37, no. 6, pp. 1119–1132, Jun. 2018.

[32] T.-W. Huang, T.-Y. Ho, and K. Chakrabarty, "Reliability-oriented broadcast electrode-addressing for pin-constrained digital microfluidic biochips," in *Proc. IEEE/ACM Int. Conf. Computer-Aided Design (ICCAD)*, San Jose, CA, USA, Nov. 2011, pp. 448–455.

[33] S.-H. Yeh, J.-W. Chang, T.-W. Huang, S.-T. Yu, and T.-Y. Ho, "Voltage-aware chip-level design for reliability-driven pin-constrained EWOD chips," *IEEE Trans. Comput.-Aided Design Integr. Circuits Syst.*, vol. 33, no. 9, pp. 1302–1315, Sep. 2014.

[34] S.-T. Yu, S.-H. Yeh, and T.-Y. Ho, "Reliability-driven chip-level design for high-frequency digital microfluidic biochips," *IEEE Trans. Comput.-Aided Design Integr. Circuits Syst.*, vol. 34, no. 4, pp. 529–539, Apr. 2015.

[35] S.-T. Yu, S.-H. Yeh, and T.-Y. Ho, "Reliability-driven chip-level design for high-frequency digital microfluidic biochips," in *Proc. Int. Symp. Phys. Design (ISPD)*, 2014, pp. 133–140.

[36] Y. Zhao, T. Xu, and K. Chakrabarty, "Broadcast electrode-addressing and scheduling methods for pin-constrained digital microfluidic biochips," *IEEE Trans. Comput.-Aided Design Integr. Circuits Syst.*, vol. 30, no. 7, pp. 986–999, Jul. 2011.

[37] J. L. Gross and J. Yellen, "Graph theory and its applications," *Math. Gazette*, vol. 84, p. 499, Mar. 2005.

[38] O. Keszocze, P. Niemann, A. Friedemann, and R. Drechsler, "On the complexity of design tasks for digital microfluidic biochips," *Microelectron. J.*, vol. 78, pp. 35–45, Aug. 2018.

[39] E. Tomita, A. Tanaka, and H. Takahashi, "The worst-case time complexity for generating all maximal cliques and computational experiments," *Combinatorics Probab. Comput.*, vol. 1, pp. 161–170, Aug. 2004.

[40] A. Singh, N. Singh, T. Jindal, A. Rosado-Muñoz, and M. K. Dutta, "A novel pilot study of automatic identification of EMF radiation effect on brain using computer vision and machine learning," *Biomed. Signal Process. Control*, vol. 57, Mar. 2020, Art. no. 101821.

[41] Y. Barash, G. Guralnik, N. Tau, S. Soffer, T. Levy, O. Shimon, E. Zimlichman, E. Konen, and E. Klang, "Comparison of deep learning models for natural language processing-based classification of non-English head CT reports," *Neuroradiology*, vol. 62, no. 10, pp. 1247–1256, Oct. 2020.

[42] S. A. Valizadeh, R. Riener, S. Elmer, and L. Jäncke, "Decrypting the electrophysiological individuality of the human brain: Identification of individuals based on resting-state EEG activity," *NeuroImage*, vol. 197, pp. 470–481, Aug. 2019.

[43] M. Roimi, A. Neuberger, A. Shrot, M. Paul, Y. Geffen, and Y. Bar-Lavie, "Early diagnosis of bloodstream infections in the intensive care unit using machine-learning algorithms," *Intensive Care Med.*, vol. 46, no. 3, pp. 454–462, Mar. 2020.

[44] D. Kringel, G. Geisslinger, E. Resch, B. G. Oertel, M. C. Thrun, S. Heinemann, and J. Lötsch, "Machine-learned analysis of the association of next-generation sequencing–based human TRPV1 and TRPA1 genotypes with the sensitivity to heat stimuli and topically applied capsaicin," *PAIN*, vol. 159, no. 7, pp. 1366–1381, Jul. 2018.
[45] Q. Wang, W. He, H. Yao, T.-Y. Ho, and Y. Cai, "SVM-based routability-driven chip-level design for voltage-aware pin-constrained EWOD chips," in *Proc. Symp. Int. Symp. Phys. Design (ISPD)*, 2015, pp. 49–56.
[46] T. Joachims, "Making large-scale SVM learning practical," in *Advances in Kernel Methods: Support Vector Learning*, B. Scholkopf, C. Burges, and A. Smola, Eds. Cambridge, MA, USA: MIT Press, 1999.

JINLONG SHI received the bachelor's and master's degrees from the Harbin University of Science and Technology, in 2010 and 2013, respectively. He is currently pursuing the Ph.D. degree with the School of Electronics and Information Engineering, Harbin Institute of Technology, Harbin, Heilongjiang, China. His main research interests include automatic test and control technology, microfluidic chip technique, digital microfluidic chip technology, and so on.

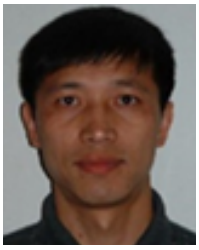

PING FU (Member, IEEE) received the Ph.D. degree from the Harbin Institute of Technology, in 1999. He is currently a Professor with the School of Electronics and Information Engineering, Harbin Institute of Technology, Harbin, Heilongjiang, China. His main research interests include artificial intelligence, image processing, compressive sensing, and automatic test technology.

WENBIN ZHENG (Member, IEEE) received the Ph.D. degree from the Harbin Institute of Technology, Harbin, Heilongjiang, China, in 2014. He is currently a Lecturer with the School of Electronics and Information Engineering, Harbin Institute of Technology. His main research interests include digital microfluidic technology, artificial intelligence, cooperative transmission, wireless sensor, networks, and automatic test and control technology.